

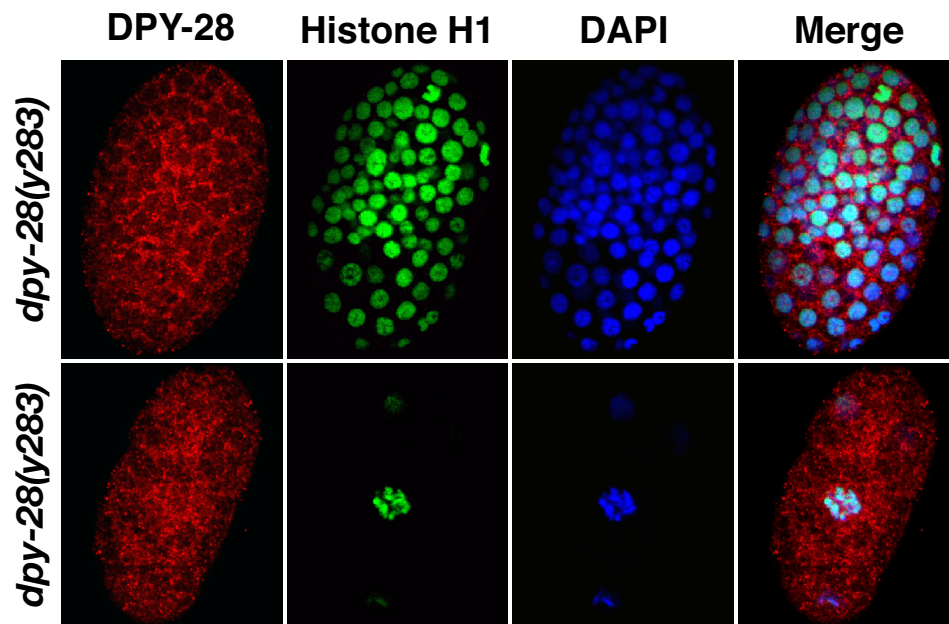
## Supplementary Information

### Meiotic crossover number and distribution are regulated by a dosage compensation protein that resembles a condensin subunit

Chun J. Tsai, David G. Mets, Michael R. Albrecht, Paola Nix, Annette Chan, and Barbara J. Meyer

Howard Hughes Medical Institute, Department of Molecular and Cell Biology, University of California, Berkeley, CA 97420, USA

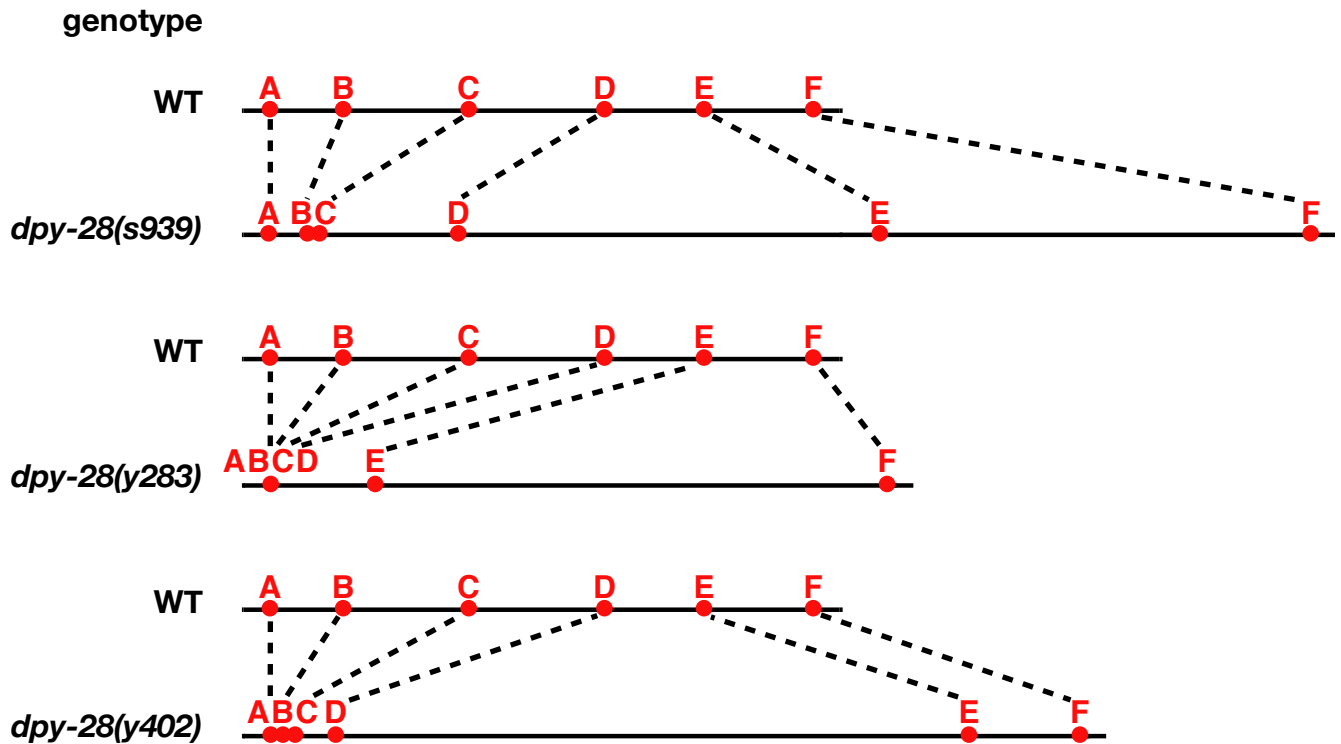
### Supplementary Figure 1



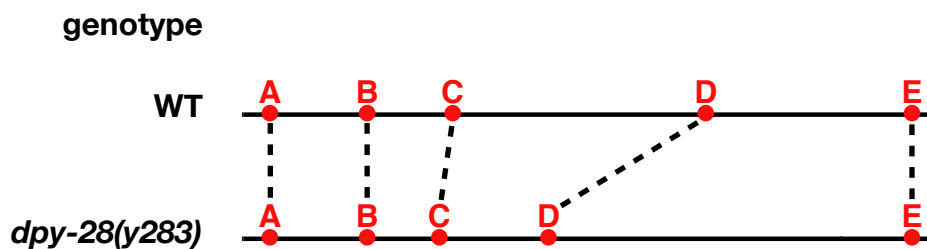
Supplementary Figure 1. In *dpy-28(y283)* mutants, both the X staining pattern and mitotic chromosome staining pattern of DPY-28 antibodies are absent. Shown are false-colored confocal images of *dpy-28(y283)* XX embryos co-stained with DAPI (blue) and antibodies to DPY-28 (red) and histone H1 (green).

## Supplementary Figure 2

### Chromosome X genetic maps

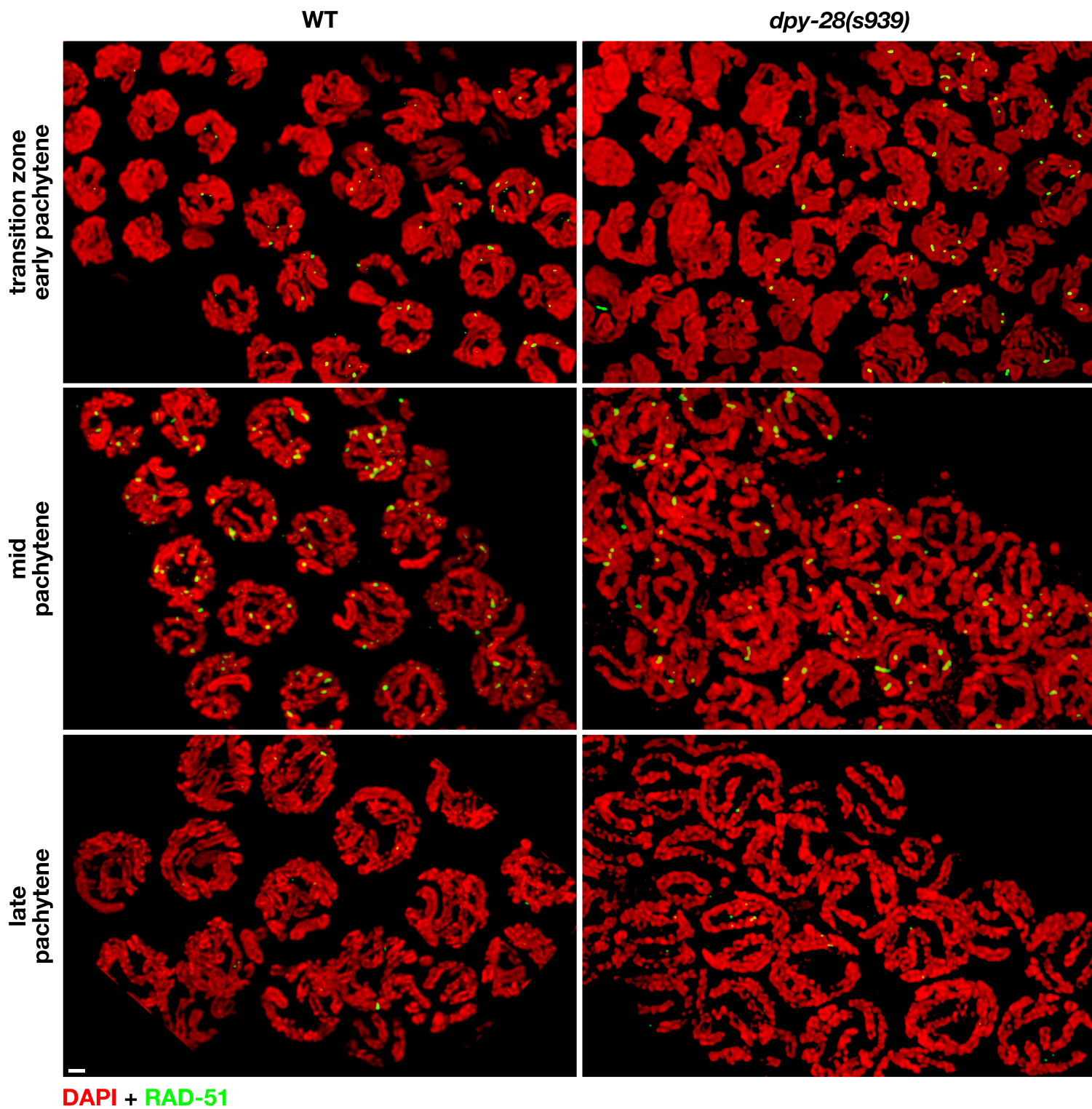


### Chromosome I genetic maps



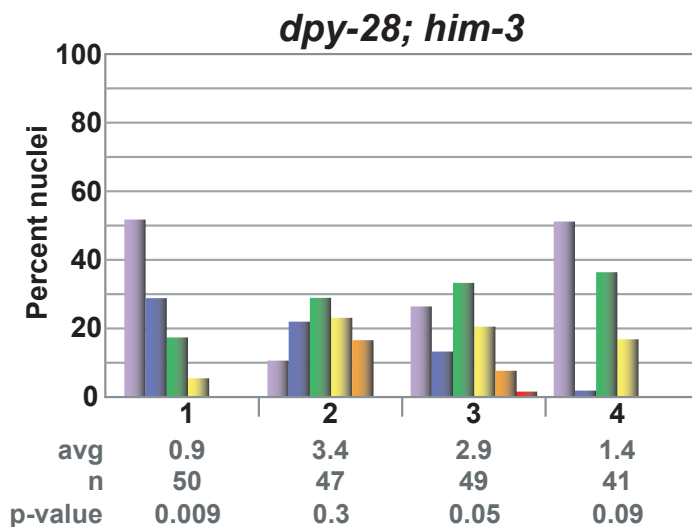
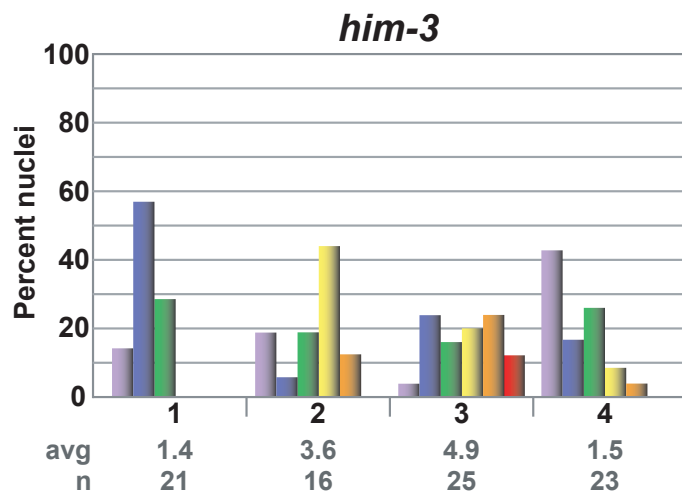
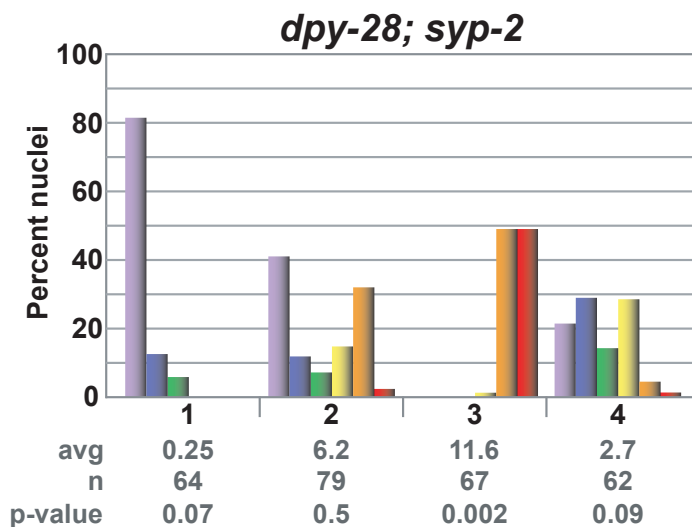
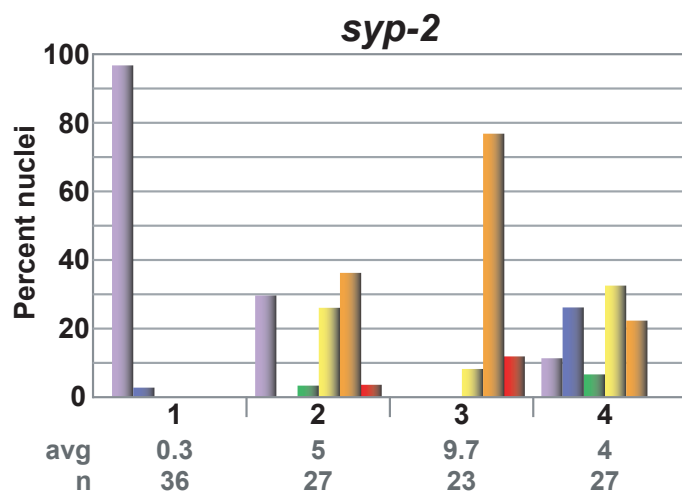
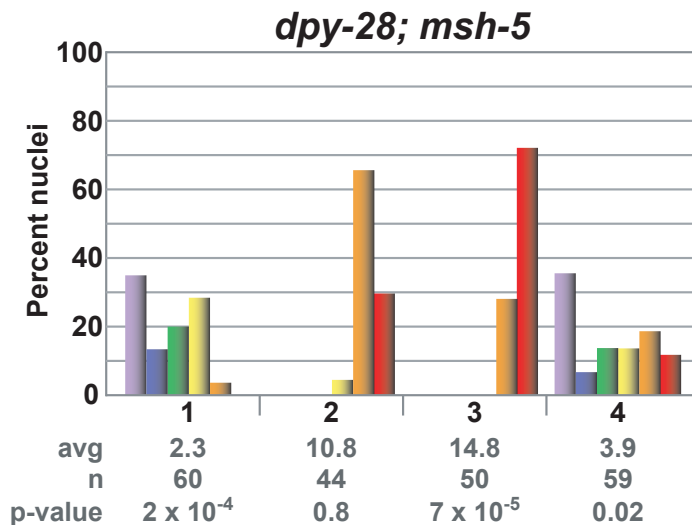
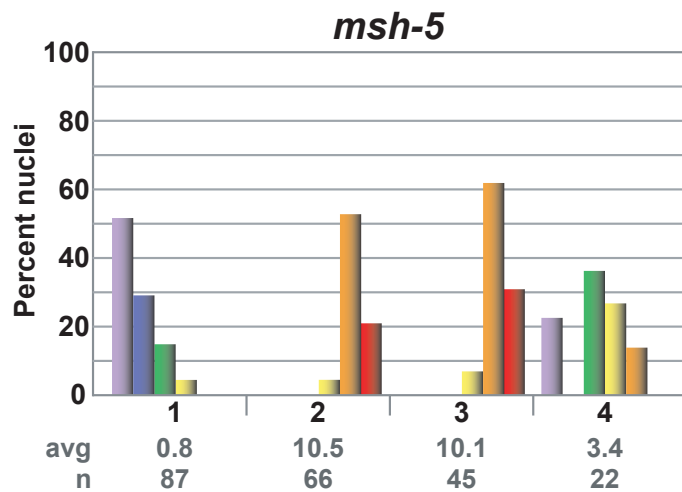
Supplementary Figure 2. Genetic map expansion and contraction caused by *dpy-28* mutations. Shown are the comparisons of genetic maps between wild-type and *dpy-28* animals for chromosomes X and I. The intervals and the recombination frequencies used to draw the maps are from Fig. 4.

### Supplementary Figure 3



Supplementary Figure 3. *dpy-28* mutants exhibit an increase in DSB-dependent early recombination intermediates (RAD-51 foci) but normal progression of focus appearance and disappearance. All panels are false-color confocal images of wild-type or *dpy-28(s939)* germlines stained with RAD-51 antibodies (green) and DAPI (red). In wild-type animals, RAD-51 foci first appear in the transition zone, peak in early to mid-pachytene, and disappear by pachytene exit. In *dpy-28* mutant gonads, more RAD-51 foci occur per nucleus, but the progression resembles that of wild-type animals. Gonads were scanned at high resolution with a confocal microscope, and the images were subjected to Huygens Essential (Scientific Volume Imaging) deconvolution software. Scale bars, 1  $\mu\text{m}$ .

## Supplementary Figure 4

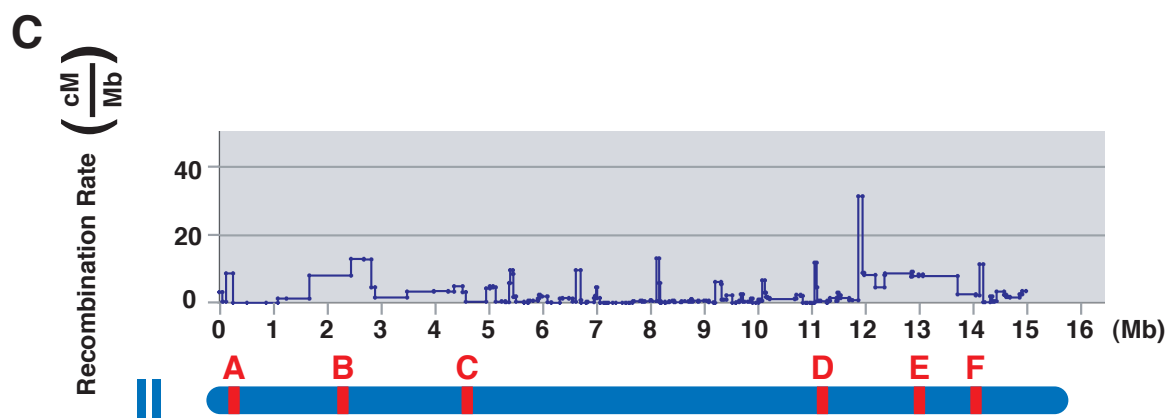
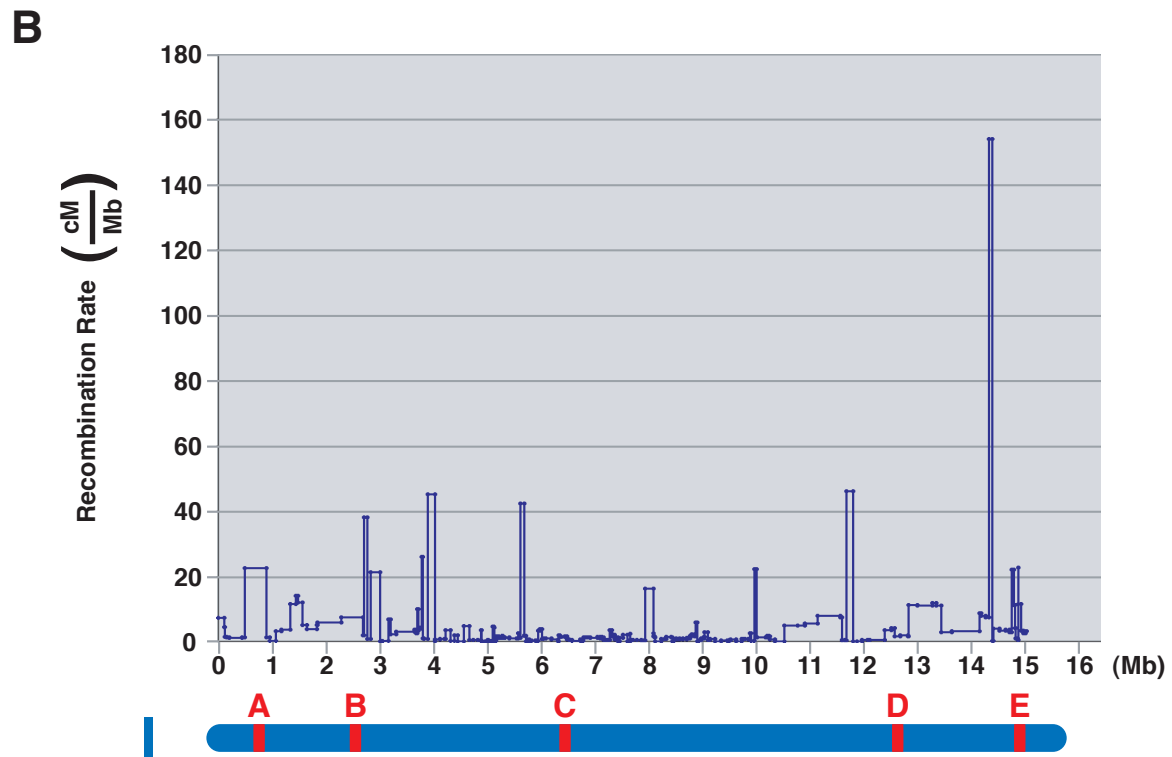
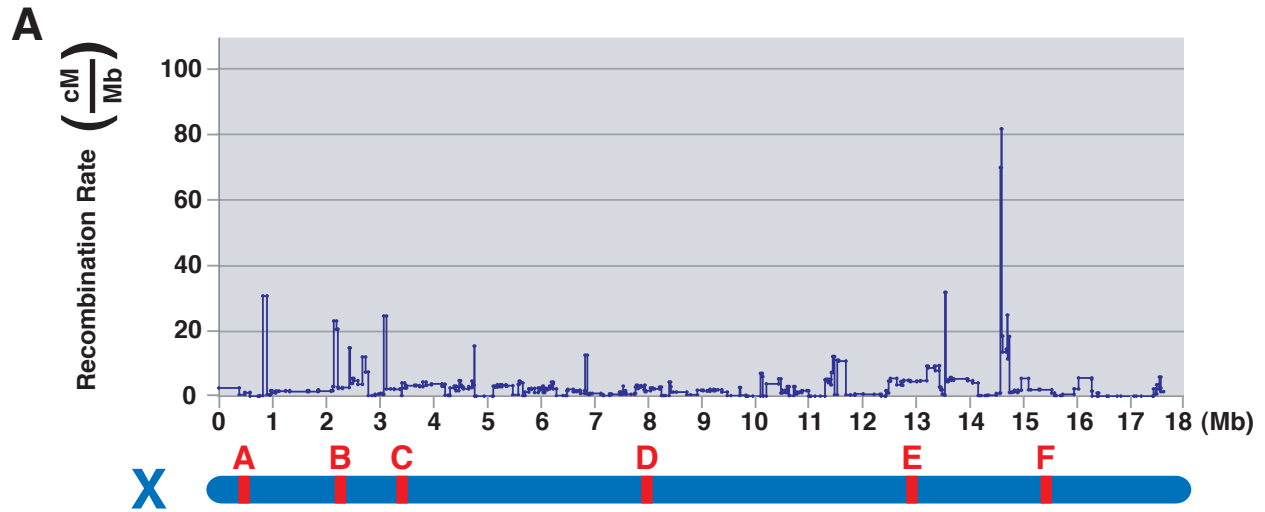


RAD-51 foci/nucleus: 0 1 2-3 4-6 7-12 >12

Supplementary Figure 4. *dpy-28* mutants require MSH-5 and SYP-2 for the timely resolution of RAD-51-bound recombination intermediates and HIM-3 for the increase in RAD-51 foci. Histograms depicting quantification of RAD-51 foci in *msh-5*, *syp-2*, and *him-3* single mutants compared to *dpy-28*; *msh-5*, *dpy-28*; *syp-2*, and *dpy-28*; *him-3* double mutants. Each column color represents a class of nuclei with the indicated number of RAD-51 foci. The *y* axis shows the percentage of nuclei in each class. The *x* axis shows the position along the germline. For each genotype, gonads from the end of the premeiotic region to the beginning of diplotene were divided into four equal regions (1-4 on the histograms) for quantifying RAD-51 foci. This division strategy was necessary because not all genotypes have equal sizes of transition zones and pachytene regions. *syp-2* mutants have an extended transition zone, and *him-3* mutants have almost no transition zone. In the histograms, *n* is the number of nuclei scored, and *avg* is the average number of RAD-51 foci per nucleus. MSH-5, a protein required to resolve recombination intermediates into COs, and SYP-2, an SC central region component, are essential for the timely resolution of RAD-51 foci. In mutants depleted of either protein, RAD-51 foci persist into late pachytene, but disappear in the last five rows of late pachytene nuclei (our results and Carlton et al. 2006). Images in Fig. 7A,B were taken from the beginning of late pachytene. If *dpy-28* mutations merely caused delayed resolution of early recombination intermediates, we would expect to find a similar accumulation of unresolved RAD-51 foci in pachytene (regions 2 or 3) of *dpy-28*; *msh-5* compared to *msh-5* and *dpy-28*; *syp-2* compared to *syp-2*. *p*-values from  $\chi^2$  tests show that the number of RAD-51 foci is significantly increased in region 3 of *dpy-28*; *msh-5* compared to *msh-5* and *dpy-28*; *syp-2* compared to *syp-2*. These results indicate that the

increase in RAD-51 foci most plausibly reflects an increase in DSB formation. The increase in RAD-51 foci in *dpy-28* mutants does require the axis protein HIM-3, which is critical for organizing meiotic chromosomes. p-values from  $\chi^2$  tests show that the number of RAD-51 foci in regions 2 and 3 (0.3 and 0.05, respectively) are not different between *dpy-28; him-3* and *him-3*.

# Supplementary Figure 5



Supplementary Figure 5. Recombination rate variation along chromosomes X, I and II in wild-type worms. (A, B, C) Shown are calculated recombination rates (Y axis) plotted against the physical distance from the left end of chromosomes X, I and II (X axis). Approximate physical positions of the snip-SNP markers used for crossover analysis are shown below graphs. The recombination rate is defined as (genetic interval)/(physical interval) and calculated based on cloned genes annotated in WormBase (<http://www.wormbase.org>, release WS158, 2006). For this study, 332, 242 and 196 cloned genes were used on chromosomes X, I and II, respectively. Crossover activities are higher around the distal one third of the chromosome and lower near the center. Crossover hotspots are noted as higher peaks. The genetic intervals that were expanded in *dpy-28* animals correlate with the chromosomal regions that harbor crossover hotspots.

### **Supplementary Movie Legends**

Supplementary Movie 1. QuickTime movie showing a false colored wild-type pachytene nucleus stained with antibodies to RAD-51 (green) and the axis protein HTP-3 (red). The nucleus was scanned at high resolution using a confocal microscope, and the images were subjected to Huygens Essential deconvolution software.

Supplementary Movie 2. QuickTime movie showing a false colored *dpy-28(s939)* pachytene nucleus stained with antibodies to RAD-51 (green) and the axis protein HTP-3 (red). The nucleus was scanned at high resolution using a confocal microscope, and the images were subjected to Huygens Essential deconvolution software.

Supplementary Table 1

snip-SNP markers used in recombination analysis of *dpy-28*

LG	snip-SNP	cosmid	map position	primer sequence (5' → 3')	restriction enzyme	N2 restriction fragments (bp)	CB4856 restriction fragments (bp)
X	A	F28C10	-19	GGTATCCGATCCCTTCAACAAG TGGCAAAACACATCCCTGTG	<i>Bsp</i> HI	208, 156	364
X	B	EGAP7	-15.5	AGAATCTGGGAGGTAAATGG CCCATTGAAACTACTCCACCTG	<i>Sfc</i> I	700, 246	577, 369
X	C	F11D5	-11.1	TCGTGGCACCATAAAAGTG GATTCAGATCAAACAGAGGTGG	<i>Dra</i> I	243	128, 115
X	D	F45E1	-0.76	GGTTCCTGGACGATAACGATGTGG TCTCTCCTCTTTCCCTCCATTCAATC	<i>Eco</i> RI	540, 228	768
X	E	C05E7	10.1	GGCTCTGAGAAACCAACAAG TGTTTGCGATGACGTGTCAG	<i>Sau</i> 3AI	318, 149	467
X	F	C33A11	20.8	CGAGCAGAGATGCAGAGTTCTCAACTG CGACCTGAAAGATGTGAGGTTCCATTATC	<i>Hae</i> III	280, 300	580
I	A	ZC123	-18.6	CCTACAACAGGCAAAGAAGC AATTCCTACCAAAGCTCCGC	<i>Ssp</i> I	643	324, 319
I	B*	Y71G12	-12.3	GACAATGACCAATAAGACG GATCCGTGAAATTGTTCCG	<i>Bsr</i> I	440, 125	364, 125, 76
I	B	F32B5	-7.7	TAATGTACCACCTCACGTGACG CTTTCACCAGAACCCTCTATTC	<i>Sfu</i> I	348	188, 160
I	C	K04F10	0.9	ATCATTCTCCAGGCCACGTTAC CTGAACTAGTCGAACAAACCCC	<i>Nde</i> I	594	300, 294
I	D	T07D10	13.6	CTTGGTGTGGGGAGAATATAGG TTGTCCGGATTGACTCTGC	<i>Sau</i> 3AI	303, 63	207, 96, 63
I	E	ZK909	28.8	CACAAGTGGTTTGGAAGTACCG CAACAAAGGGATAGATCACGGG	<i>Hind</i> III	450	236, 214
II	A	T25D3	-17.9	CGGAGATAGTCTCGTGGTACTG CAGTCATGCTCCAAACATTCTC	<i>Dra</i> I	336, 93	288, 93, 48
II	B	R52	-14.5	TCCATCTTCGCAATCAGATTTC AACGTA CTGCTTCCCATGCTC	<i>Alu</i> I	368	203, 165
II	C	M03A1	-4	TCATCTGTCGAGTGCTTTTG CGATCGCTCAAATGGTTG	<i>Taq</i> I	291, 81, 80	210, 81, 80, 70
II	D	F37H8	3.3	TTCTCACAATTCTTTTCCAAG TTCATA TTTCCCTCGCTGG	<i>Taq</i> I	572, 112, 15	382, 190, 112, 15

### Supplementary Table 1

II	E	Y38F1	13.6	TAGGAAAGTTGTGTCCACCTGG TGATGACTCCTTCTTCAGCTGC	<i>Hinf</i> I	449	288, 160
II	F	Y51H1	20.9	GATTCGGAATGGGTGTTG TCTTGAATGCGTGGTGTG	<i>Taq</i> I	482	340, 142

---

Shown are snip-SNP markers, their map positions, primer pairs used for PCR, restriction enzymes to digest PCR fragments, and diagnostic restriction fragments for the N2 and CB4856 alleles. The snip-SNP markers can be found in Wormbase, <http://www.wormbase.org>, release WS158, 2006 and Wicks et al. 2001.

## Supplementary Table 2

### Meiotic crossing over on chromosome X in wild-type animals and *dpy-28* mutants

Genotype	3-CO	2-CO	1-CO	0-CO	n	RF <sup>a</sup>	2-CO ratio <sup>b</sup>	3-CO ratio <sup>c</sup>	Coefficient of coincidence		p-value <sup>f</sup>
									<sup>d</sup> chromosome wide (intervals 1-4 vs. 5)	<sup>e</sup> for highest 2-CO intervals (4 + 5)	
control	0	0	42	52	94	0.45	0	0	0	0	-
<i>dpy-28(s939)/+</i>	7	16	41	30	94	1.0	0.25	0.11	1.0	2.4	<10 <sup>-6</sup>
<i>dpy-28(s939)</i>	3	14	40	35	92	0.83	0.25	0.053	1.0	1.4	<10 <sup>-4</sup>
<i>dpy-28(y283)/+</i>	0	0	49	47	96	0.51	0	0	0	0	0.4
<i>dpy-28(y283)</i>	0	0	36	33	69	0.52	0	0	0	0	0.3
<i>dpy-28(y402)/+</i>	1	3	54	36	94	0.67	0.052	0.017	0.72	1.2	0.015
<i>dpy-28(y402)</i>	0	4	43	29	76	0.67	0.085	0	1.0	1.1	0.013
<i>dpy-28(y284)/+</i>	0	0	40	55	95	0.42	0	0	0	0	0.7
<i>dpy-28(y284)</i>	0	0	46	48	94	0.49	0	0	0	0	0.6

3-CO, triple crossover; 2-CO, double crossover; 1-CO, single crossover; 0-CO, no crossovers  
 Intervals and positions of 2-COs and 3-COs are defined in Supplementary Table 3.

$$^a \left( \frac{\text{total number of crossover events}}{\text{number of meiotic products analyzed}} \right)$$

$$^b \left( \frac{\text{number of 2-COs}}{\text{number of 1-COs} + \text{2-COs} + \text{3-COs}} \right)$$

$$^c \left( \frac{\text{number of 3-COs}}{\text{number of 1-COs} + \text{2-COs} + \text{3-COs}} \right)$$

$$^d \left( \frac{\text{number of observed 2-COs involving interval 1-4 and interval 5}}{(\text{frequency of 1-COs in 1-4}) (\text{frequency of 1-COs in 5}) (\text{number of scored chromatids})} \right)$$

$$^e \left( \frac{\text{number of observed 2-COs involving intervals 4 and 5}}{(\text{frequency of 1-COs in 4}) (\text{frequency of 1-COs in 5}) (\text{number of scored chromatids})} \right)$$

<sup>f</sup> p-value from the chi<sup>2</sup> test reflects the difference in distribution of single and multiple crossovers between control and mutant animals.

### Supplementary Table 3

#### Six-marker recombination analysis of the X chromosome

Recombinant interval	Marker Configuration (A-B-C-D-E-F)	<i>unc-32</i> + (Control)	<i>unc-32 dpy-28 (s939)</i> +	<i>unc-32 dpy-28 (s939) dpy-28 (s939)</i>
0-CO	B-B-B-B-B-B H-H-H-H-H-H	51	30	35
1 (A-B)	B-H-H-H-H-H H-B-B-B-B-B	2	9	1
2 (B-C)	B-B-H-H-H-H H-H-B-B-B-B	13	13	1
3 (C-D)	B-B-B-H-H-H H-H-H-B-B-B	13	8	7
4 (D-E)	B-B-B-B-H-H H-H-H-H-B-B	9	5	15
5 (E-F)	B-B-B-B-B-H H-H-H-H-H-B	5	6	14
2 + 3	B-B-H-B-B-B H-H-B-H-H-H	0	1	0
2 + 5	B-B-H-H-H-B H-H-B-B-B-H	0	3	0
3 + 4	B-B-B-H-B-B H-H-H-B-H-H	0	2	1
3 + 5	B-B-B-H-H-B H-H-H-B-B-H	0	0	1
4 + 5	B-B-B-B-H-B H-H-H-H-B-H	0	10	12
1 + 3 + 4	B-H-H-B-H-H H-B-B-H-B-B	0	1	0
1 + 4 + 5	B-H-H-H-B-H H-B-B-B-H-B	0	0	2
2 + 3 + 4	B-B-H-B-H-H H-H-B-H-B-B	0	1	0
3 + 4 + 5	B-B-B-H-B-H H-H-H-B-H-B	0	5	1
	Total:	93	94	88

Six-marker recombination analysis of the X chromosome. X chromatids were genotyped and classified as having no crossover (0-CO); one crossover in the intervals 1, 2, 3, 4 or 5; two crossovers in the indicated pairs of intervals (2 + 3, 2 + 5, 3 + 4, 3 + 5, and 4 + 5); or three crossovers in the indicated combinations of intervals (1 + 3 + 4, 1 + 4 + 5, 2 + 3 + 4, and 3 + 4 + 5). The two possible alternative configurations of Bristol (B) and Hawaiian (H) marker alleles are indicated. Markers A–F are as defined in Figure 4. The number of chromatids in each class is shown for control, *dpy-28(s939)/+*, and *dpy-28(s939)* animals.

**Supplementary Table 4**

**Meiotic crossing over on chromosomes I and II in wild-type animals and *dpy-28* mutants**

LG	Genotype	2-CO	1-CO	0-CO	n	RF <sup>a</sup>	2-CO ratio <sup>b</sup>	Coefficient of coincidence			p-value <sup>f</sup>
								<sup>c</sup> chromosome wide intervals 1-2 vs. 3-4	<sup>d</sup> chromosome wide intervals 1-2 vs. 3-5	<sup>e</sup> highest 2-CO intervals	
I	control	1	49 (45*)	46	96	0.53 (0.49*)	0.02	0.2	-	0.6 (1+3)	-
	<i>dpy-28(s939)/+</i>	0	41 (39*)	54	95	0.43 (0.41*)	0	0	-	0	0.4
	<i>dpy-28(y283)/+</i>	1	50	45	96	0.54	0.02	0.2	-	0.6 (2+4)	1
	<i>dpy-28(y402)/+</i>	0	46*	50	96	0.48*	0	0	-	0	0.3
II	control	0	30	33	63	0.48	0	-	0	0	-
	<i>dpy-28(s939)/+</i>	1	30	36	67	0.48	0.032	-	0.3	0.5 (2+4)	0.3
	<i>dpy-28(y283)/+</i>	5	31	25	61	0.67	0.14	-	0.4	1.4 (2+4)	0.03
	<i>dpy-28(y402)/+</i>	2	42	42	86	0.53	0.045	-	0.3	2.0 (2+3)	0.2
	<i>dpy-28(y284)/+</i>	2	36	53	91	0.44	0.053	-	0.5	1.8 (1+5)	0.2

3-CO, triple crossover; 2-CO, double crossover; 1-CO, single crossover; 0-CO, no crossovers

\* denotes the experimental data obtained using snip-SNP marker B\*.

Intervals are as in Fig. 4B,C and numbered from left to right. Positions of 2-COs are shown in Supplementary Table 5.

$$a \left( \frac{\text{total number of crossover events}}{\text{number of meiotic products analyzed}} \right)$$

$$b \left( \frac{\text{number of 2-COs}}{\text{number of 1-COs + 2-COs}} \right)$$

$$c \left( \frac{\text{number of observed 2-COs involving interval 1-2 and interval 3-4}}{(\text{frequency of 1-COs in 1-2}) (\text{frequency of 1-COs in 3-4}) (\text{number of scored chromatids})} \right)$$

$$d \left( \frac{\text{number of observed 2-COs involving interval 1-2 and interval 3-5}}{(\text{frequency of 1-COs in 1-2}) (\text{frequency of 1-COs in 3-5}) (\text{number of scored chromatids})} \right)$$

$$e \left( \frac{\text{number of observed 2-COs involving intervals designated in parentheses}}{(\text{frequency of 1-COs in 1st interval}) (\text{frequency of 1-COs in 2nd interval}) (\text{number of scored chromatids})} \right)$$

<sup>f</sup> p-value from the chi<sup>2</sup> test reflects the difference in distribution of single and multiple crossovers between control and mutant animals.

## Supplementary Table 5

### 2-COs of chromosome I

Recombinant interval	$\frac{\pm}{+}$ (Control)	$\frac{dpy-28(y283)}{+}$
1 (A-B) + 3 (C-D)	1	0
2 (B-C) + 4 (D-E)	0	1
Total:	96	96

2-COs of chromosome I are shown in the indicated pairs of intervals. Markers A–E are as defined in Figure 4. The number of chromatids in each class is shown for control, and *dpy-28(y283)/+* animals.

### 2-COs of chromosome II

Recombinant interval	$\frac{\pm}{+}$ (Control)	$\frac{dpy-28(s939)}{+}$	$\frac{dpy-28(y283)}{+}$	$\frac{dpy-28(y402)}{+}$	$\frac{dpy-28(y284)}{+}$
1 (A-B) + 2 (B-C)	0	0	1	0	0
1 (A-B) + 5 (E-F)	0	0	0	0	1
2 (B-C) + 3 (C-D)	0	0	0	2	0
2 (B-C) + 4 (D-E)	0	1	3	0	0
2 (B-C) + 5 (E-F)	0	0	0	0	1
4 (D-E) + 5 (E-F)	0	0	1	0	0
Total:	63	67	61	86	91

2-COs of chromosome II are shown in the indicated pairs of intervals. Markers A–F are as defined in Figure 4. The number of chromatids in each class is shown for control, *dpy-28(s939)/+*, *dpy-28(y283)/+*, *dpy-28(y402)/+*, and *dpy-28(y284)/+* animals.

## Supplementary Materials and Methods

### *Strains used in the study*

The following strains were used: wild-type (N2 Bristol), *dpy-28(s939)/qC1 dpy-19(e1259) glp-1(q339)[qIs26] III*, *dpy-28(y283)/qC1 dpy-19(e1259) glp-1(q339)[qIs26] III*, *dpy-28(y284)/qC1 dpy-19(e1259) glp-1(q339)[qIs26] III*, *dpy-28(y402)/qC1 dpy-19(e1259) glp-1(q339)[qIs26] III*, *dpy-28(s939) III*; *him-5(e1490) V*, *dpy-28(s939)/qC1 dpy-19(e1259) glp-1(q339)[qIs26] III*; *spo-11(ok79) IV/nT1[unc(n754) let] IV;V*, *spo-11(me44) IV/nT1[unc(n754) let qIs50] IV;V*, *dpy-28(s939) III*; *spo-11(me44) IV/nT1[unc(n754) let qIs50] IV;V*, *dpy-28(s939)/qC1 dpy-19(e1259) glp-1(q339)[qIs26] III*; *msh-5(me23) IV/nT1[unc(n754) let] IV;V*, *dpy-28(s939)/qC1 dpy-19(e1259) glp-1(q339)[qIs26] III*; *him-3(gk149) IV/nT1[qIs51] IV;V*, *dpy-28(s939)/qC1 dpy-19(e1259) glp-1(q339)[qIs26] III*; *syp-2(ok307) V/nT1[unc(n754) let(m435)] IV;V*, *dpy-28(s939)/vab-7(e1562) III*; *him-17(ok424) V*, *unc-32(e189) dpy-27(y167) III*; *flu-2(e1003) xol-1(y9) V*, *dpy-26(n199) unc-30(e191) IV*; *lon-2(e678) xol-1(y9) V*, *him-8(e1489) IV*; *yIs34 (xol-1::gfp) V*, *spo-11(ok79) IV/nT1[unc(n754) let] IV;V*, *msh-5(me23) IV/nT1[unc(n754) let] IV;V*, *him-3(gk149) IV/nT1[qIs51] IV;V*, *syp-2(ok307) V/nT1[unc(n754) let(m435)] IV;V*, *him-17(ok424) V/nT1 IV;V*, *her-1(hv1y101) V*; *xol-1(y9) sdc-2(y74) unc-9(e101) X*, *her-1(e1520) sdc-3(y126) V*; *xol-1(y9) X*, and *sdc-1(n485) X*.

### *Screens for dpy-28 mutations*

The non-complementation screen was performed by mating groups of hermaphrodites of genotype *dpy-28(y1) vab-7(e1562)*; *flu-2(e1003) xol-1(y9) unc-3(e151)* grown at 15° C with wild-type males mutagenized with EMS according to standard procedures. Matings

were transferred every 24 hr. Candidate F1 Unc non-Vab animals were picked to individual plates and mated with wild-type males at 20° C. F2 wild-type hermaphrodite animals were picked from plates with wild-type male siblings and allowed to self. Those that failed to produce F3 Vab progeny were presumed to carry a new *dpy-28* mutation. F3 wild-type hermaphrodites, presumably heterozygous for a new *dpy-28* mutation, were mated with *eT1/unc-49(e382) vab-7(e1562)* males. F4 progeny were picked and allowed to self. F5 progeny were examined for the presence of *eT1* homozygotes, which are Unc. Wild-type siblings of F5 Unc progeny were picked as potential maternally rescued *dpy-28* homozygotes. The F6 progeny of the cloned F5 hermaphrodites were examined for the presence of Dpy phenotypes. This procedure resulted in two *dpy-28* mutations, *y283* and *y284*.

Brood counts of mutants revealed that only 0.5% of *y283* XX animals are viable, and *y283* produces 5.6% spontaneous males through X nondisjunction. Almost all *y283* XX mutants die prior to the L2 stage. In contrast, 22% of *y284* XX animals are viable, and *y284* produces only 0.5% spontaneous males. *y284* XX escapers are Dpy, and *y284* XO animals appear wild type. The strengths of the *y283* and *s939* alleles are similar; *y284* resembles *yIts* (Plenefisch et al. 1989).

A frozen *C. elegans* deletion library was screened using PCR to obtain the deletion allele *y402*. Outside primers used were PD15/PD16 and inside primers used were PPD17/PD18 below. No *y402* XX mutants are viable and *y402* produces 7% spontaneous males through X nondisjunction.

### *Genetic mapping of dpy-28*

Since *cul-1* is sterile, *cul-1(e1756) + vab-7(e1562)/+ unc-47(e307) vab-7(e1562)* hermaphrodites were mated to *dpy-28(y1)* males to generate F1 *cul-1(e1756) + vab-7(e1562)/+ dpy-28(y1)* + heterozygous hermaphrodites. Potential Vab non-Cul recombinants were picked from plates that had siblings with the *cul-1 vab-7* chromosome. Progeny from each of the potential recombinants were picked to isolate Vab non-Cul hermaphrodites homozygous for the recombinant chromosome. Hermaphrodites that segregated no Cul animals were scored as homozygous recombinants. Since *dpy-28* is maternally rescued, progeny of the homozygous recombinant animals were examined for the Dpy phenotype to determine if the *dpy-28(y1)* mutation was present in the recombinant chromosome.

### *RFLP analysis of dpy-28*

Recombinants were generated by mating male AB1 animals with hermaphrodite *unc-49(e382) dpy-28(y1) vab-7(e1562)* animals. Heterozygous F1 animals were picked to individual plates and transferred every 24 hr. F2 Unc non-Vab and Vab non-Unc recombinants were picked. F3 animals from these recombinants were picked to isolate homozygous recombinants. A total of 26 Unc non-Vab and 2 Vab non-Unc recombinants were isolated (Table 5). Unc non-Vab animals were isolated more frequently because Vab animals are sick. Genomic DNA from the recombinants was prepared according to standard methods. Gels were transferred for Southern analysis according to standard methods, with the exception that the gel was washed in 0.25N HCl for 20 min prior to denaturation to aid the transfer of high molecular weight DNA. Probes were made using random priming from cosmid DNA previously digested with *HindIII* or *EcoRI*. Blots were probed overnight at 65° C, and the results examined by autoradiography.

*cDNA identification for RNAi assays to define dpy-28*

To isolate cDNAs from the *dpy-28* region, we used the *C. elegans* genome consortium release of partial YAC Y39A1 sequence, shown by Southern analysis to span the *dpy-28* region. Specifically, 529 kb of partial Y39A1 sequence was split into 20kb fragments, which were used in blastn searches of the dbest library to identify expressed sequence tags (ESTs) of cDNAs in the *dpy-28* region. This method yielded 238 cDNAs, which were organized into cDNA families representing a single gene using the ESTs in blastn searches of the dbest library to identify other ESTs that overlapped with the query EST. This approach reduced the candidate cDNAs to 50 independent families. The cDNA families were further reduced by eliminating families that contained significant homology to proteins unlikely to be *dpy-28*. A total of 33 potential *dpy-28* cDNA families remained. 33 individual EST clones were chosen to represent the 33 potential *dpy-28* cDNA families in the RNA interference assay.

All cDNAs used in the RNA interference assay were derived from the Yuji Kohara cDNA library. All RNA interference experiments were performed with single-stranded anti-sense RNA. To generate anti-sense RNA from the cDNA clones, the cDNA clones were excised as bluescript derived phagemids according to the Lambda ZAP II Kit (Stratagene). RNA was made using RiboMAX Large Scale RNA Production System (Promega). RNA (100 µg/ml-1 mg/ml) was injected directly into the gonads of *unc-76(e911) sdc-3(y52)/sdc-3(y128)* young adult hermaphrodites. Injected animals were cloned and transferred every 24 hr. The *unc-76(e911) sdc-3(y52)* progeny were examined for the presence of male tail structures. Only qualitative differences in the proportion of Unc hermaphrodites were scored in the original screen.

Progeny were quantified from a second round of injections into *unc-76(e911) sdc-3(y52)/sdc-3(y128)* animals with RNAs derived from yk32e9, the positive control *dpy-26*, and the two negative controls yk3c1 and yk3b1. Injections with the RNAs resulted in the following ratios of Unc Tra males to Unc hermaphrodites, respectively: *dpy-26* RNA, 22 to 133; yk32e9 RNA, 11 to 83; yk3b1 RNA, 145 to 2 Unc, and yk3c1 RNA, 288 to 5. In addition to the strong suppression of the Tra phenotype, treatment with yk32e9 RNA resulted in a high degree of lethality and dumpiness. Furthermore, 3 spontaneous wild-type males were observed on these plates, strongly suggesting that the dumpiness was karyotype specific.

#### *Sequence identification of dpy-28 mutations*

Genomic DNA of *dpy-28* mutants was prepared and sequenced using standard techniques. Exons five to sixteen were amplified by PCR in four separate primer reactions; MA-62/MA-65, MA-66/MA-67, MA-48/MA-71 and MA-72/MA-85. Four separate MA-48/MA-71 PCR reactions were sequenced with primers MA-69 and MA-52, which identified a 195 nucleotide deletion in the 10th exon of *dpy-28(s939)*. To identify the molecular lesions in *y283* and *y284*, genomic fragments about 3-5 kb in length were obtained by single worm PCR from the respective *dpy-28* mutant. Regions corresponding to predicted exons were directly sequenced by automated sequencing. The allele *dpy-28(y1)* caused a G to A transition, resulting in G1078E.

#### *List of primers used*

The following primers were used for sequence analysis and PCR.

MA-48	TACCGAACGAAGAGAATCAGTG
MA-51	ACAAC TTTGCTAACAAGTGACG
MA-52	ATGATCCCAGAAAGAAGATGGCTC
MA-56	CGATTGGGGTTCTTCGGCGTTTG

MA-58 TGATTAATTGTTGAACTTGAGC  
 MA-62 CACTTGCAATAAATGTTACG  
 MA-65 CGATTTTCTCAGAAAAACTG  
 MA-66 GCTTTTAATACAGTACTCTTG  
 MA-67 GGAGAAATTCGATTTTTTGCAG  
 MA-69 GTGTTGCACAATACGCATTCTC  
 MA-71 CTGGAAAAAAAAAGCCGCGAATC  
 MA-72 CATTTCCAAAACGAA GTTTC  
 MA-85 AGTAATAAAAGACGATGGTAC  
 SL-1 TCTAGAATTCCTCGGTTTAATTACCCAAGTTTG  
 SL-2 TCTAGAATTCCGCGGTTTAAACCCAGTTACTC  
 PD15 GGACCTTTAAAAGCGGCAATTG  
 PD16 CAAACGGCTGATTTCTTGTTG  
 PD17 CGGATTTGCCTGATTTTTTCC  
 PD18 GGAGTAGCGCCAGTGGGGAAA

*Antibody preparation*

A DNA fragment encoding DPY-28 amino acids 351-771 was cloned into pRSET (Invitrogen), adding six histidines to the N-terminus. Recombinant protein was induced in *E. coli* BL21pLysS cells and purified by nickel-chelate chromatography and SDS-PAGE. Rabbit and rat anti-sera were purified against the fusion protein as in Lane and Harlow (1982).

*Immunoprecipitation and immunoblot analysis*

To prepare whole-cell extracts from wild-type and *dpy-28(s939); him- 5(e1490)* mutants, embryos were collected from bleached hermaphrodites grown in liquid culture. Prior to

bleaching, gravid hermaphrodites were separated from embryos and larvae in the culture medium by passing cultures through a 35 mm Nitex filter. Embryos were stored at -80°C in 1:1 volumes in radioimmunoprecipitation assay buffer (10 mM Na-Phosphate pH 7.0, 150 mM NaCl, 1% Nonidet P-40, 1% sodium deoxycholate, 2 mM EDTA, protease inhibitors [1 mM phenylmethylsulfonyl fluoride, 10  $\mu$ M benzamidine, 5  $\mu$ M phenanthroline, and 0.5  $\mu$ g each of antipain, leupeptin, pepstatin, aprotinin, and chymostatin per ml]). In preparing extracts, materials were kept at 4°C at all times. Embryos (~0.5 g) were thawed under tap water, spun briefly in a microcentrifuge, homogenized using a mini-homogenizer and then sonicated. Sonicated material was centrifuged at 14,000 rpm for 15 min, and the supernatant was saved. Protein quantitation was performed using Bradford reagent (BioRad).

To prepare crude lysates from wild-type and *dpy-28* mutant gravid hermaphrodites, 500 gravid hermaphrodites of each genotype were picked, washed twice with M9 minimal medium, spun down in a microcentrifuge, and resuspended in 1X SDS sample buffer with 7 M urea. The samples were then boiled for 10 min.

For immunoprecipitation, wild-type and *dpy-28(s939); him-5(e1490)* embryonic extracts were preincubated with protein A beads at 4°C for 1 hr and centrifuged at 14,000 rpm for 2 min. 4  $\mu$ g of affinity-purified anti-DPY-28 antibodies were then added to the supernatant and incubated at 4°C for 1 hr. After incubation, protein A beads were added to capture the antibody-protein complexes for 30 min at 4°C with rocking.

Immunoprecipitates were washed three times with radioimmunoprecipitation assay buffer (10 min each), subjected to SDS-PAGE on a 7% acrylamide gel, and transferred to an Immobilon-P transfer membrane (Millipore). Proteins were incubated with primary

antibodies and then visualized with the appropriate secondary antibodies using Chemiluminescence Reagent Plus (NEN).

### *Immunostaining*

Nematode strains for examining DPY-28 localization in embryos are as described in Lieb et al. (1996). The strain *him-8(e1489); yIs34 (xol-1::gfp)* was used to discriminate between XO and XX embryos because it produces a fusion protein containing GFP and the first 89 amino acids of XOL-1 exclusively in XO embryos.

Immunostaining of embryos was performed as described in Dawes et al. (1999). The following dilutions of antibodies were used: rabbit anti-DPY-28 1:50 to 1:100, rat anti-DPY-28 1:50, rabbit anti-XOL-1 1:50 to 1:100, rabbit anti-DPY-26 1:100.

Germline immunofluorescence and FISH staining were performed and imaged as described in Howe et al. (2001). FISH probes were to 5S rDNA on chromosome V and to right-end X locus (340 kb from end) that contained repeats of sequence GACTCCATCCACCAGCACTGCTTCGAGTACGACAGAAAGCACTTC. The detailed protocol is as follows. For germline staining, adult worms were picked into 5  $\mu$ l of sperm salts (50 mM PIPES, pH 7.0, 25 mM KCl, 1 mM MgSO<sub>4</sub>, 45 mM NaCl, and 2 mM CaCl<sub>2</sub>) on a positively charged glass slide. An incision was made in each worm between the pharynx and gonad using a syringe needle (Precision Glide, Becton Dickinson & Co., 22 G 1 1/2) to release the internal organs. Approximately 5  $\mu$ l of paraformaldehyde of concentrations ranging from 2 to 4% (Electron Microscopy Sciences) dissolved in sperm salts were added, and the slide was incubated in a humid chamber for 2 to 5 min. An 18 X 18 mm coverslip was placed over the worms, and the slide was frozen on a block of dry ice for at least 10 min. Once the slide was retrieved

from the dry ice, the coverslip was quickly removed with a sharp stroke of a single-edged razor blade. The slide was placed immediately into 95% ethanol for 1 min, washed three times (each for at least 10 min) in PBST (1 X PBS, 0.5% Triton X-100, and 1 mM EDTA, pH 8), and the PBST was wicked off without allowing the worms to dry. Next, 25  $\mu$ l primary antibody diluted in PBST was placed on the worms, and the worms were covered gently with a 20 X 20 mm piece of parafilm and incubated overnight at room temperature in a humid chamber. The slide was then incubated three times (at least 10 min each) in PBST, the PBST was wicked off, and 25  $\mu$ l of secondary antibody was added. The worms were covered with a 20 X 20 mm piece of parafilm and incubated 8 hr to overnight in a humid chamber. The slide was washed three times (at least 10 min each) in PBST, the PBST was wicked off, and 10  $\mu$ l of DAPI (1  $\mu$ g/ ml) was added. The slide was mounted with 20  $\mu$ l DABCO (0.1 g/ml DABCO in 0.1 X PBS and 90% glycerin), covered with a 22 X 40 mm coverslip, and sealed with nail polish. These specimens were visualized with a Leica TCS NT confocal microscope. For pachytene nuclei stained with antibodies to RAD-51 and HTP-3, the nuclei were scanned at high resolution with a confocal microscope, and the images were subjected to Huygens Essential (Scientific Volume Imaging) deconvolution software.

#### *DAPI analysis*

The DAPI bodies were counted by eye on the Zeiss Axioplan 2 using the 100X Plan-Apochromat 1.4 NA objective and scanning in Z. Diakinesis images were collected on the Leica SP2 in stacks taken every 0.3 microns and projected using ImageJ.

### *Time course analysis for RAD-51 foci*

RAD-51 foci were quantified in germline nuclei of age-matched hermaphrodites, using a Leica SP2 confocal microscope. At least 2 full gonads were imaged and analyzed.

Germlines were divided into five zones, beginning from the distal tip: the premeiotic zone was defined as the region before crescent shape morphology, the TZ was the region with crescent morphology, and pachytene was the region after crescent morphology, and was divided evenly into three regions based on length.

### **References**

- Carlton, P.M., Farruggio, A.P., and Dernburg, A.F. 2006. A link between meiotic prophase progression and crossover control. *PLoS Genet.* **2**: e12.
- Dawes, H.E., Berlin, D.S., Lapidus, D.M., Nusbaum, C., Davis, T.L., and Meyer, B.J. 1999. Dosage compensation proteins targeted to X chromosomes by a determinant of hermaphrodite fate. *Science* **284**: 1800-1804.
- Howe, M., McDonald, K.L., Albertson, D.G., and Meyer, B.J. 2001. HIM-10 is required for kinetochore structure and function on *Caenorhabditis elegans* holocentric chromosomes. *J. Cell Biol.* **153**: 1227-1238.
- Lane, D. and Harlow, E. 1982. Two different viral transforming proteins bind the same host tumour antigen. *Nature* **298**: 517.
- Lieb, J.D., Capowski, E.E., Meneely, P., and Meyer, B.J. 1996. DPY-26, a link between dosage compensation and meiotic chromosome segregation in the nematode. *Science* **274**: 1732-1736.
- Plenefisch, J.D., DeLong, L., and Meyer, B.J. 1989. Genes that implement the hermaphrodite mode of dosage compensation in *Caenorhabditis elegans*. *Genetics* **121**: 57-76.
- Wicks, S.R., Yeh, R.T., Gish, W.R., Waterston, R.H., and Plasterk, R.H. 2001. Rapid gene mapping in *Caenorhabditis elegans* using a high density polymorphism map. *Nat Genet* **28**: 160-164.